

DESIGN AND ANALYSIS OF AN UNMANNED UNDERWATER VEHICLE: UNSTIFFENED AND T RING STIFFENED STRUCTURE CONFIGURATION

B. Venkata Rao¹ Assistant Professor, Mechanical & WISTM Engineering College

Sahoo. Navjeet² Mechanical & WISTM Engineering College

G. Gyana Shekar³ Mechanical & WISTM Engineering College

ABSTRACT

The structural integrity of unmanned underwater vehicles (UUVs) subjected to high hydrostatic pressure presents a significant challenge in marine engineering. This study conducts a comparative finite element analysis of unstiffened and T-ring stiffened hull configurations. Using ANSYS, the models evaluate stress distribution, deformation behavior, and buckling resistance. Aluminium Alloy AA7068 is selected for its high strength-to-weight ratio, with Retrogression and Re-Aging (RRA) heat treatment applied to enhance corrosion resistance and durability. Results demonstrate that the T-ring stiffened configuration markedly improves structural performance over the unstiffened model, offering increased stiffness, reduced deformation, and substantially enhanced buckling resistance under external pressure. Compared to flat stiffeners, T-stiffeners provide superior load distribution and overall structural stability. The numerical outcomes align closely with analytical predictions, validating the modeling approach. This study underscores the effectiveness of T-ring stiffening in developing robust, lightweight UUV structures optimized for demanding deep-sea environments.

KEY WORDS: *Underwater vehicle, Design, Stiffeners, Hydrostatic pressure, Static structural, Buckling factor*

1. INTRODUCTION

Unmanned underwater vehicles (UUVs) are increasingly employed in advanced marine operations such as deep-sea exploration, military reconnaissance, and subsea infrastructure inspection, all of which require reliable structural performance under extreme hydrostatic pressures. The pressure hull must resist collapse, minimize deformation, and ensure operational safety, making structural optimization critical. Cylindrical shells are commonly used for hull construction due to their efficient stress distribution; however, unstiffened shells are susceptible to buckling under external pressure. To improve rigidity and stability, stiffeners are incorporated, with T-ring stiffeners offering superior structural efficiency by increasing the moment of inertia and enhancing load distribution relative to simpler stiffening methods. This

study presents a comprehensive 3D modeling and finite element analysis of a UUV hull, comparing unstiffened and T-ring stiffened configurations using ANSYS. The investigation focuses on stress distribution, deformation behavior, and buckling resistance under high-pressure conditions. Aluminium Alloy AA7068 is selected for its excellent strength-to-weight ratio, complemented by Retrogression and Re-Aging (RRA) heat treatment to improve corrosion resistance and durability in harsh marine environments. The primary objective is to quantify the structural benefits of T-ring stiffening over unstiffened designs. Findings demonstrate that T-ring stiffeners markedly enhance stiffness, reduce deformation, and improve buckling resistance, thereby advancing the development of safer and more efficient underwater vehicle structures.

2. LITERATURE REVIEW

i. S. Margonis

Focused on multi-objective optimization in AUV design, useful for selecting optimal dimensions (L/D ratio), weight, and performance trade-offs in your UUV.

ii. **T.-H. Joung, K. Sammut, F. He, S.-K. Lee** Applied CFD-based shape optimization, helping improve hydrodynamic efficiency and reduce drag in your vehicle design.

iii. Z. Sun, G. Hu, X. Nie, J. Sun

Provides detailed buckling analysis of cylindrical shells, directly relevant for evaluating pressure hull stability under external hydrostatic pressure.

iv. M. W. Temme

Compares analytical and numerical failure methods, supporting validation of your ANSYS results with theoretical approaches.

v. S. Timoshenko, S. Woinowsky-Krieger

Fundamental theory of plates and shells; essential for deriving stress, deformation, and buckling equations used in your design.

vi. P. A. Rometsch et al.

Explains heat treatment of 7xxx aluminium alloys, useful for understanding strength enhancement of AA7068 material used in your hull.

vii. J. Osten et al.

Focuses on precipitation behavior of AA7068, helping justify material selection based on high strength and corrosion resistance.

viii. E. H. Baker et al. (NASA Shell Analysis Manual)

Provides standard procedures for shell stress and buckling analysis, supporting your structural calculations and validation.

ix. N. Wakita et al.

Describes deep-sea AUV development, useful for understanding real-world design constraints and pressure resistance requirements.

x. E. H. Baker et al. (NASA CR-912)

Extended shell analysis reference, helpful for advanced failure prediction and design safety factors.

xi. Y. Nie et al.

Discusses motion performance in turbulent conditions, useful for stability and control considerations of your UUV.

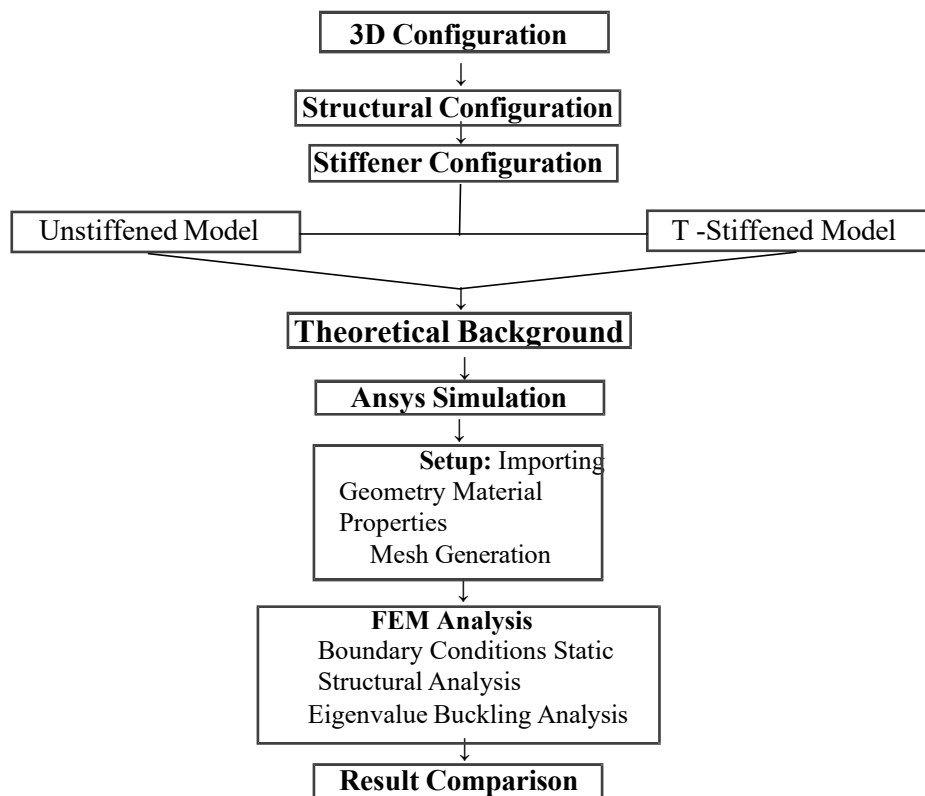
xii. M. Helal, H. Huang, D. Wang, E. Fathallah

Studies sandwich composite pressure hulls, providing insights into lightweight structural design and enhanced strength-to-weight ratio, useful for comparing metallic and composite hull performance in your project.

xiii. X. Li

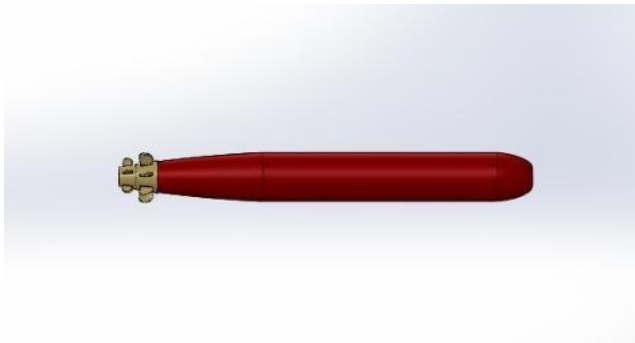
Focuses on strength and stability of ring-stiffened cylindrical shells, directly applicable for understanding how stiffeners improve buckling resistance and structural integrity of your pressure hull.

3. METHODOLOGY



4. STRUCTURAL CONFIGURATION

Unmanned Underwater Vehicle



The unmanned underwater vehicle consists of three main structural elements: the forward section, a T-ring stiffened cylindrical shell, and the tail section. Together, they form the primary load-bearing system designed to withstand hydrostatic pressure at a depth of 1500 meters. The design balances strength, rigidity, and hydrodynamic efficiency. The cylindrical shell acts as the main pressure-resistant component, while the forward and tail sections ensure smooth geometric transitions and efficient load distribution. T-ring stiffeners enhance the hull's ability to resist external pressure and improve structural resilience.

Forward Section

The forward section has a tapered conical shape that reduces hydrodynamic drag and promotes smooth fluid flow. Its curved surface enables uniform pressure distribution, minimizing stress concentrations. It also ensures a seamless connection with the cylindrical shell, supporting effective load transfer and maintaining structural integrity.

Cylindrical Shell

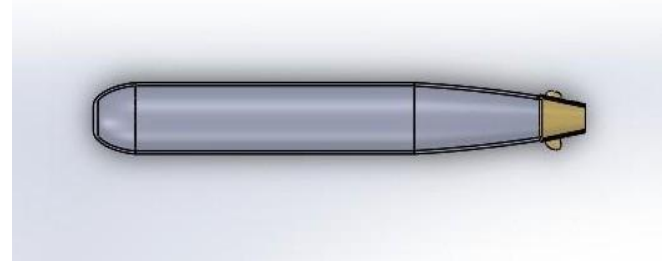
The cylindrical shell serves as the primary load-bearing component engineered to resist external hydrostatic pressure. Reinforcement is provided by T-ring stiffeners strategically positioned along its length, which significantly increase the shell's moment of inertia. This enhancement leads to improved stiffness and greater resistance to deformation. The addition of T-stiffeners optimizes load distribution and delays the onset of buckling—a critical failure mode in deep-sea conditions. Compared to unstiffened and flat-stiffened designs, the T-ring stiffened shell exhibits superior structural behavior, with reduced deformation and increased stability under high-pressure environments.

Tail Section

The tail section features a tapered conical profile that minimizes drag and flow separation. It ensures smooth structural continuity from the cylindrical shell and supports efficient load transfer. Additionally, it accommodates propulsion and control systems, meeting both structural and functional requirements.

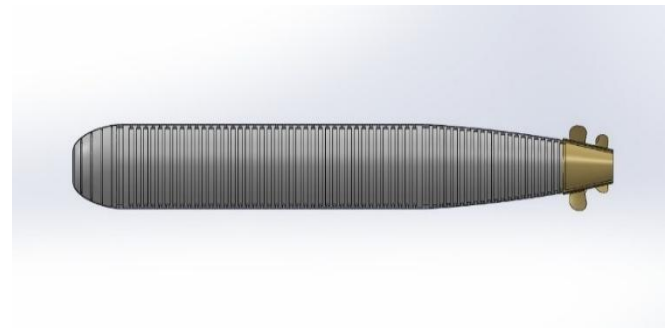
5. STIFFENER CONFIGURATIONS

Unstiffened Model



The unstiffened configuration serves as a baseline model to evaluate structural behavior without reinforcement, enabling clear identification of inherent limitations and comparison with stiffened designs. The forward section is defined by its conical geometry, reflecting natural load distribution under external pressure. The cylindrical shell is modeled as a thin-walled structure to assess stiffness, deformation, and susceptibility to instability. The tail section is a tapered extension that ensures smooth load transfer and maintains structural continuity along the vehicle.

T-Stiffened Model



The T-stiffened configuration represents the most advanced reinforcement approach in this study, offering high structural rigidity and improved resistance to instability under external pressure. The forward section retains its original geometry, ensuring smooth load transfer to the reinforced region. The cylindrical shell is strengthened with T-section ring stiffeners, which increase the section modulus through the combined action of the flange and web. This leads to better load distribution and enhanced buckling resistance. The tail section integrates with the stiffened shell, providing a gradual stiffness transition and maintaining overall structural balance.

6. THEORETICAL BACKGROUND

Stress Analysis Using Von Mises Yield Criterion

a) A **closed conical shell** subjected to external hydrostatic pressure.

The equivalent Von Mises stress is expressed as:

$$= \frac{\sqrt{3}}{2} \cdot \frac{r}{h \sin}$$

b) The cylindrical shell is analysed using thin shell theory under external pressure.

Hoop stress = $\frac{p r}{h}$

Axial stress = $\frac{p r}{2h}$

The equivalent Von Mises stress is given by:

$$= \sqrt{3} \cdot \frac{p r}{2h}$$

c) The tail section is treated as an **inclined open conical shell**

$$= \frac{\sqrt{3}}{4h \cos}$$

Buckling Assessment Based on Stress Ratio

The buckling factor (λ) is evaluated as:

- Ratio of material yield strength to induced Von Mises stress
- = /

Interpretation

- $\lambda > 1$ → Structure is safe
- $\lambda \approx 1$ → Critical condition
- $\lambda < 1$ → Failure (buckling likely) Application to

forward section and Tail section

- The Von Mises stress obtained from analysis is used
- The ratio with yield strength gives an estimate of buckling resistance
- This provides a quick and effective design validation tool

Buckling Analysis of Stiffened Cylindrical Shell

For the cylindrical shell reinforced with stiffeners, buckling behaviour becomes more complex and is categorized into distinct modes. Analytical methods are employed to evaluate different instability conditions.

T-Stiffener Shell Buckling Analysis

1. Axisymmetric Mode

$$A = \frac{x \cdot \frac{h}{D}}{\sqrt{\frac{3}{4} + \epsilon_1 - \epsilon_2}}$$

- Uniform radial inward deformation
- Entire shell-stiffener system acts together

$$P_{CLB} = \frac{2.42 \cdot E \cdot \left(\frac{h}{D}\right)^{\frac{5}{2}}}{(1 - \nu^2)^{\frac{3}{4}} \left[\left(\frac{L}{D}\right) - 0.45 \cdot \left(\frac{h}{D}\right)^{\frac{1}{2}} \right]}$$

- Indicates high structural stiffness

2. Asymmetric Mode

- Non-uniform deformation with wave formation
- Sensitive to:
 - Stiffener spacing
 - Shell thickness
- Typically governs design in practical cases

3. General Instability

$$P_{CGI(n)} = \frac{E \cdot h}{R} \left[\frac{\lambda^4}{\left(n^2 + \frac{\lambda^2}{2} - 1\right) \cdot (n^2 + \lambda^2)^2} \right] + \frac{(n^2 - 1) \cdot E \cdot I_e}{R_{cg}^3 \cdot L_f}$$

- Interaction of:
 - Shell buckling
 - Stiffener bending
- Provides the lowest critical pressure in many cases
- Used as the design limiting condition.

7. ANALYSIS

Geometry Import

The three-dimensional geometry of the pressure hull, consisting of the forward section, cylindrical shell, tail section, and T-ring stiffeners, was created using CAD software and imported into ANSYS Workbench for structural analysis. Standard formats such as STEP, IGES, and Parasolid were used to ensure compatibility and accuracy during the import process. After importing, the geometry was carefully examined to eliminate gaps, overlaps, and missing surfaces. Proper connectivity between the shell and T-ring stiffeners was ensured to accurately represent load transfer and structural interaction. Minor geometric irregularities were corrected, and unnecessary small features were removed to optimize computational performance without affecting accuracy. The geometry was also verified for correct alignment and orientation to ensure proper application of loads and boundary conditions. Maintaining a clean and precise geometry is essential for achieving reliable and accurate simulation results.

Material Selection

Aluminium alloy AA7068 was chosen as the structural material due to its superior strength-to-weight ratio and excellent mechanical performance. The material provides high yield strength, enhanced stiffness, and low density, making it well-suited for deep-sea structural applications. It also offers good resistance to corrosion, which is critical in harsh marine

environments. To further improve material performance, Retrogression and Re-Aging (RRA) heat treatment is considered, enhancing resistance to stress corrosion and increasing long-term durability under high-pressure conditions. The material's good machinability supports the fabrication of complex geometries such as T-ring stiffeners and conical sections. Its established application in aerospace and high-strength engineering structures further validates its reliability for underwater vehicle design.

Mesh Generation

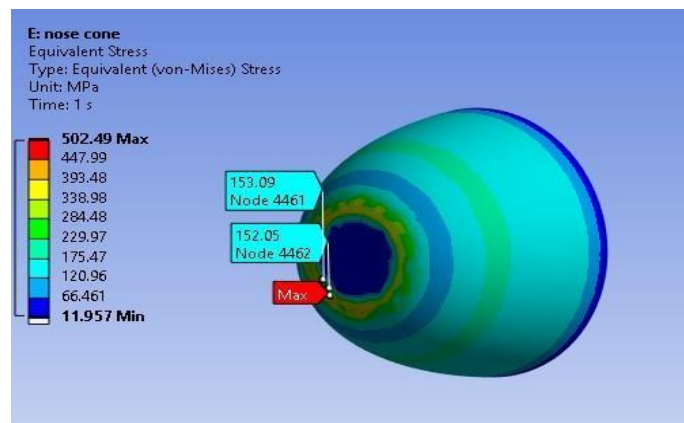
Mesh generation is an important step in finite element analysis, where the geometry is divided into smaller elements for numerical computation. In this work, tetrahedral elements were predominantly used due to the complex geometry and the presence of T-ring stiffeners. Automatic meshing with default body sizing was employed to achieve an optimal balance between computational cost and solution accuracy. Mesh quality was evaluated using parameters such as skewness, element distortion, and smooth transition between elements. Special refinement was applied near T-stiffener junctions, where stress concentration and structural interaction are significant. Mesh independence was also considered to ensure that further refinement does not significantly alter the results. A well-defined mesh improves convergence behaviour, enhances numerical stability, and ensures accurate and dependable simulation results.

7. MODEL WITH BOUNDARY CONDITIONS AND LOADS

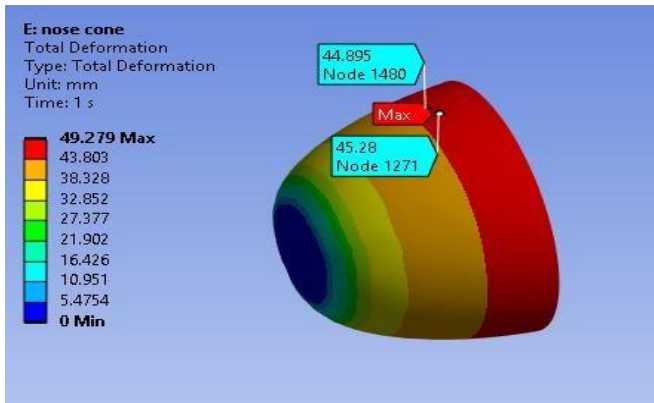
- = = = 0 at Front End And = = 0 at Rear End External Pressure $P = 15 \text{ Mpa}$ applied to the model surface
- = 1.3×10^7 at Rear End for Axial Compressive Force (SHELL)
- = 2.9×10^5 at Rear End for Axial Compressive Force (Forward & TAIL SECTION)

6. FEM ANALYSIS OF UNSTIFFENED MODEL

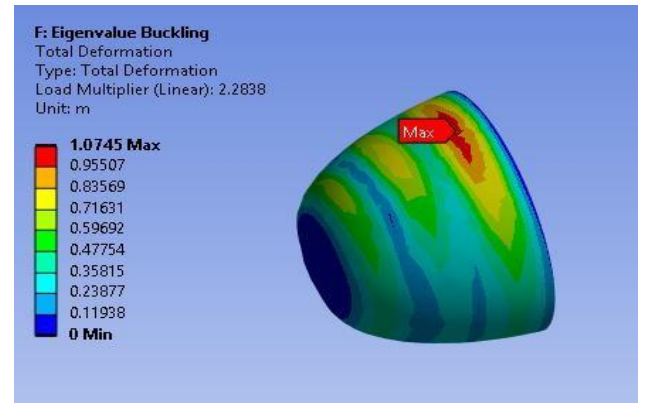
Forward Section



Maximum Equivalent Stress
153.09 Mpa

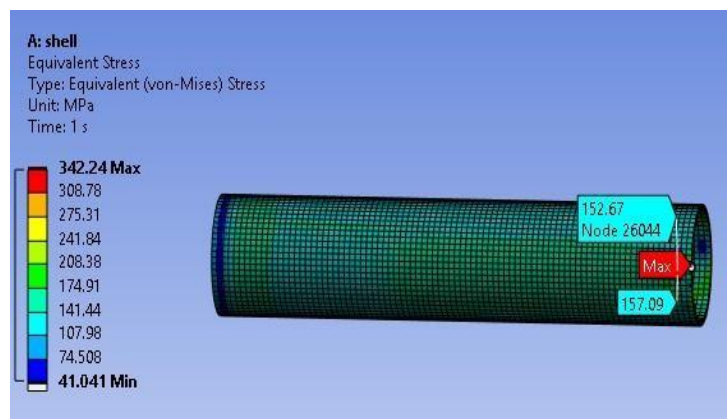


Maximum Deformation
45.28 mm

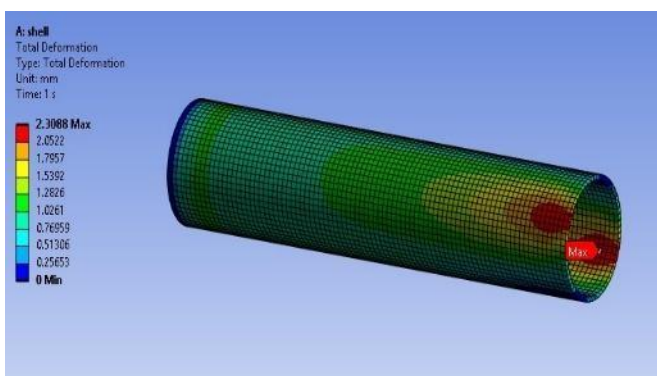


Minimum Buckling Factor
2.2

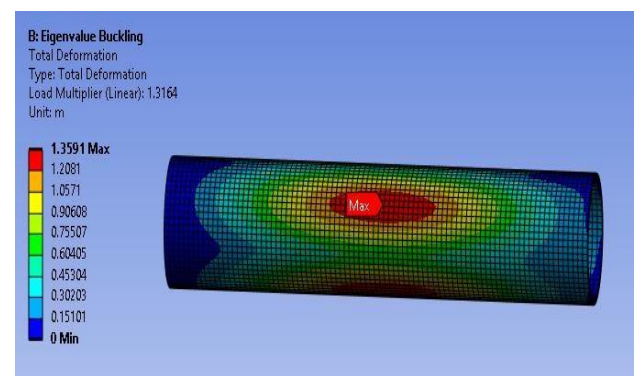
Cylindrical Shell



Maximum Equivalent Stress
157.09 Mpa

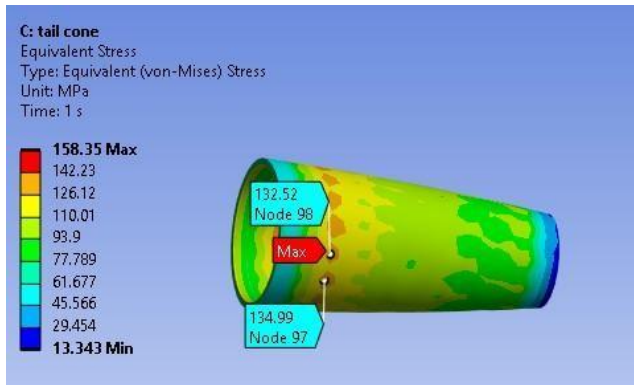


Maximum Deformation
2.3 mm

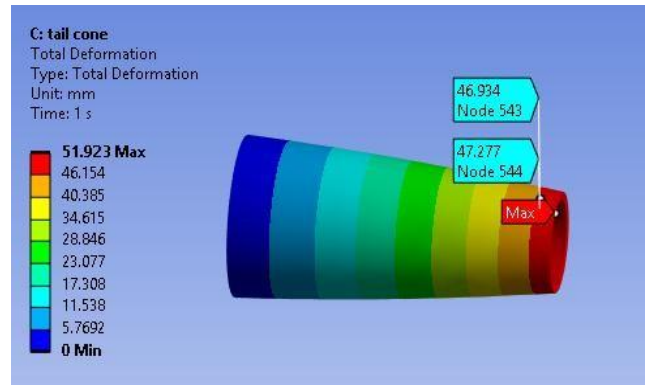


Minimum Buckling Factor
1.3

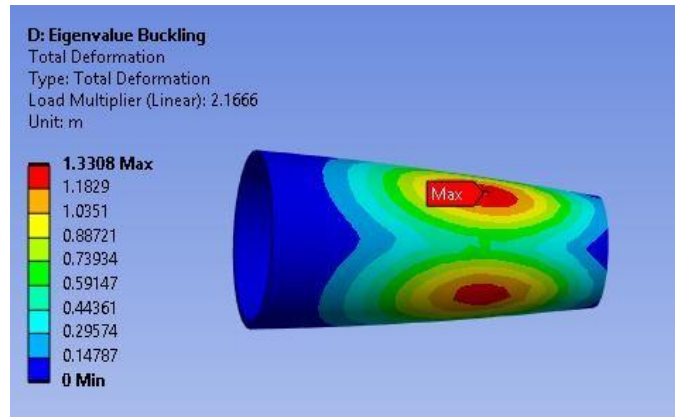
Tail section



Maximum Equivalent Stress
134.99 Mpa



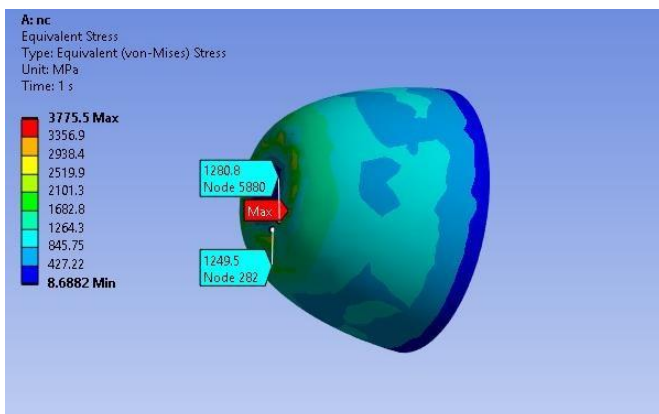
Maximum Deformation
47.27 mm



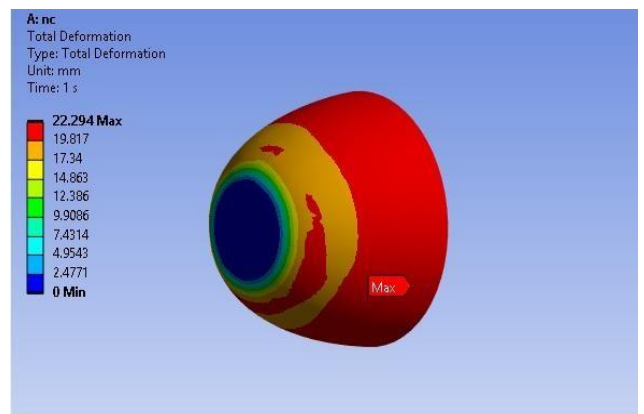
Minimum Buckling Factor 2.1

8. FEM ANALYSIS OF T STIFFENED MODEL

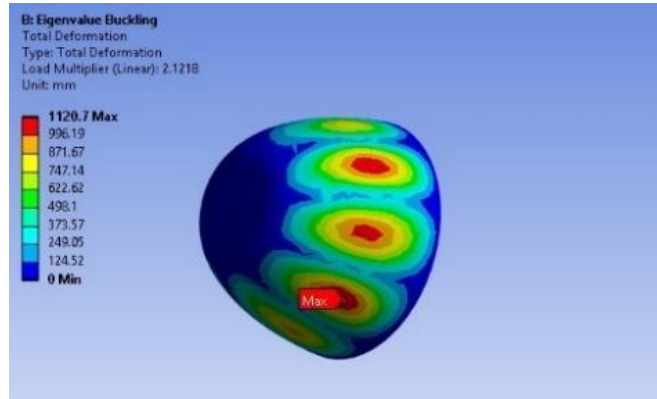
Forward Section



Maximum Equivalent Stress
1280.8 Mpa

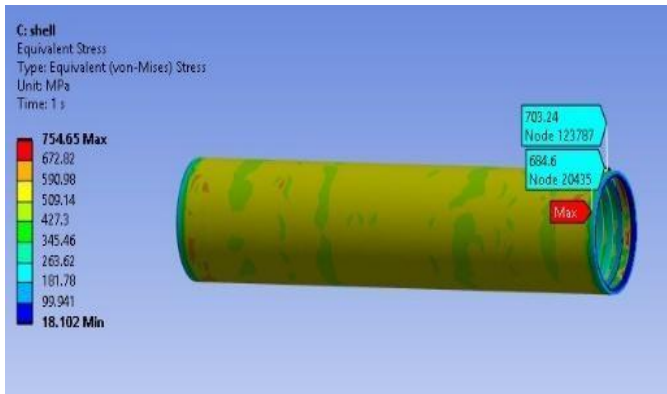


Maximum Deformation
22.29 mm

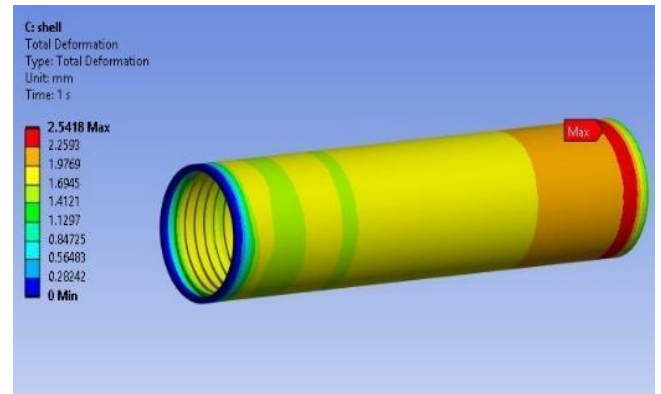


Minimum Buckling Factor 2.1

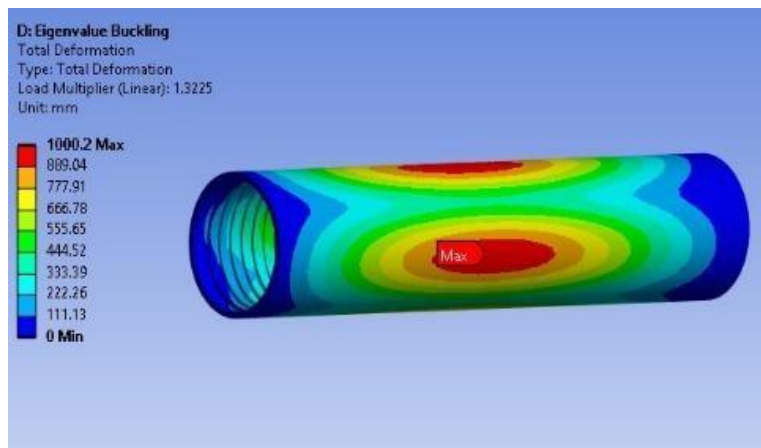
Cylindrical Shell



Maximum Equivalent Stress
703.2 Mpa

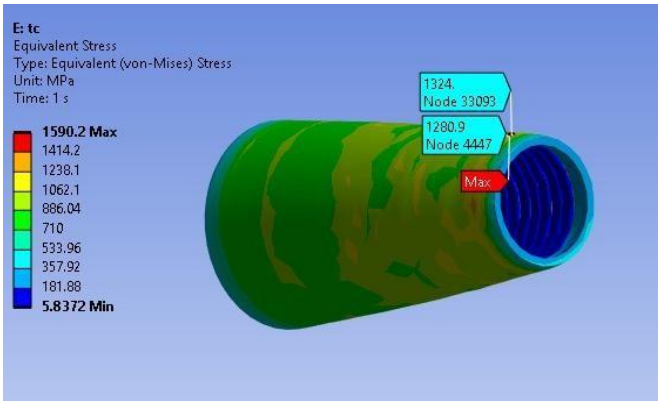


Maximum Deformation
2.54 mm

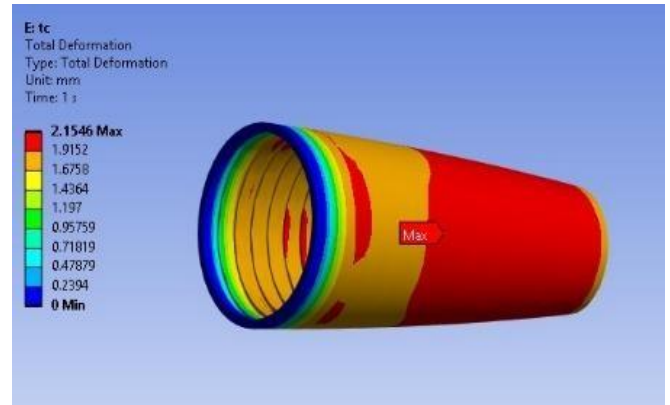


Minimum Buckling Factor 1.3

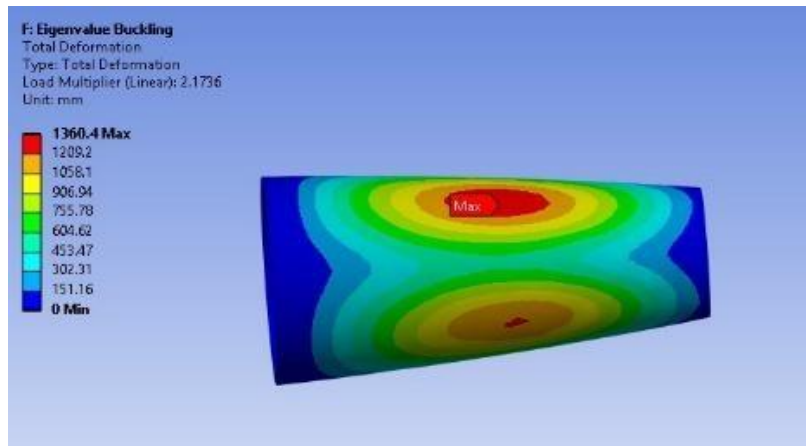
Tail section



Maximum Equivalent Stress
1324.1 Mpa

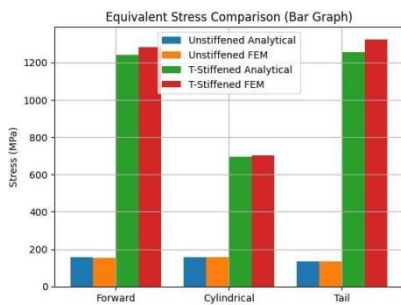


Maximum Deformation
2.15 mm

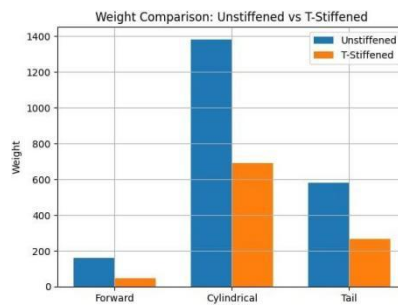


Minimum Buckling Factor 2.1

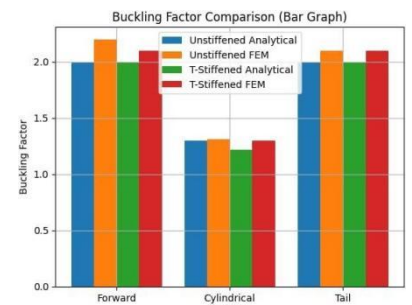
GRAPHICAL REPRESENTATION



STRESSES



WEIGHT OPTIMIZATION



BUCKLING FACTOR

RESULT

1) Comparison Of Equivalent Stresses (Von-Mises)

MODEL	PARTS	STRESSES (Mpa)	
		ANALYTICAL	FEM
UNSTIFFENED	Forward section	156.4	153.09
	Cylindrical shell	157.09	157.09
	Tail section	134.99	134.9
T STIFFENED	Forward section	1238.7	1280.8
	Cylindrical shell	695.2	703.24
	Tail section	1253.6	1324.1

2) Comparison Of Buckling Factor

MODEL	PARTS	BUCKLING FACTOR	
		ANALYTICAL	FEM
UNSTIFFENED	Forward section	2	2.2
	Cylindrical shell	1.3	1.31
	Tail section	2	2.1
T STIFFENED	Forward section	2	2.1
	Cylindrical shell	AXISYMMETRIC 1.22	1.3
		ASYMMETRIC 1.48	
		GENERAL INSTABILITY 1.10	
Tail section	2	2.1	

3) COMPARISON of WEIGHT OPTIMIZATION

TOTAL WEIGHT OPTIMIZATION (%)		
PART	REDUCTION OF WEIGHT FROM UNSTIFFENED MODEL	T STIFFENED (% REDUCED)
Forward section	159 > 45.5	71%
Cylindrical shell	1383 > 690	49%

MODEL	PARTS	WEIGHT OPTIMIZATION (kg)
UNSTIFFENED	Forward section	159
	Cylindrical shell	1383
	Tail section	580
T STIFFENED	Forward section	45.5
	Cylindrical shell	690
	Tail section	265

CONCLUSION

This study evaluates the structural response of an unmanned underwater vehicle pressure hull by comparing unstiffened and T-ring stiffened configurations using finite element analysis. Results show that the unstiffened model experiences higher deformation and lower resistance to external pressure, making it prone to buckling in deep-sea conditions. In contrast, the T-ring stiffened configuration significantly improves performance by increasing stiffness and enhancing load distribution, leading to reduced deformation and greater buckling resistance. Compared to flat stiffeners, T-ring stiffeners provide superior stability due to their higher moment of inertia and more efficient reinforcement. Stress distribution is also more uniform, reducing critical stress concentrations. The numerical results agree with analytical predictions, validating the modelling approach. Overall, T-ring stiffening proves to be an effective method for enhancing the strength, stability, and reliability of underwater vehicle structures, making it well-suited for deep-sea applications.

REFERENCE

- [1] S. Margonis, "Preliminary Design of AUV using Multi-objective Optimization."
- [2] T.-H. Joung, K. Sammut, F. He, and S.-K. Lee, "Shape Optimization of AUV using CFD."

- [3] Z. Sun, G. Hu, X. Nie, and J. Sun, “Buckling Analysis of Composite Cylindrical Shells.”
- [4] M. W. Temme, “Analytical vs Numerical Failure of Cylindrical Shells.”
- [5] S. Timoshenko and S. Woinowsky-Krieger, *Theory of Plates and Shells*.
- [6] P. A. Rometsch et al., “Heat Treatment of 7xxx Series Aluminium Alloys.”
- [7] J. Osten et al., “Heat Treatment and Precipitation Behaviour of AA 7068 Alloy.”
- [8] E. H. Baker, A. P. Cappelli, L. Kovalevsky, et al., *Shell Analysis Manual (NASA)*.
- [9] N. Wakita, K. Hirokawa, T. Ichikawa, and Y. Yamauchi, “AUV Development for Deep-Sea Exploration.”
- [10] E. H. Baker, A. P. Cappelli, L. Kovalevsky, F. L. Rish, and R. M. Verette, *Shell Analysis Manual (NASA CR-912)*.
- [11] Y. Nie, D. Song, Z. Wang, Y. Huang, and H. Yang, “Design and Motion Performance of Turbulent AUV Platform.”
- [12] M. Helal, H. Huang, D. Wang, and E. Fathallah, “Sandwich Composite Pressure Hull Analysis.”
- [13] X. Li, “Strength and Stability of Ring-Stiffened Cylindrical Shells.”